Technical Report
RAL-TR-95-028

Radiative Parton Model Analysis of Polarized Deep Inelastic Lepton Nucleon Scattering

M Glück E Reya and W Vogelsang

July 1995

COUNCIL FOR THE CENTRAL LABORATORY OF THE RESEARCH COUNCILS

Enquiries about copyright, reproduction and requests for
additional copies of this report should be addressed to:

The Central Laboratory for the Research Councils
Library and Information Services
Rutherford Appleton Laboratory
Chilton
Didcot
Oxfordshire
OX11 0QX
Tel: 01235 445384   Fax: 01235 446403
E-mail library@rl.ac.uk

ISSN 1358-6254

DO-TH 95/11
RAL-TR-95-028
July 1995

Radiative Parton Model Analysis of Polarized Deep Inelastic Lepton Nucleon Scattering

M. Glück, E. Reya

Universität Dortmund, Institut für Physik,
D-44221 Dortmund, Germany

W. Vogelsang

Rutherford Appleton Laboratory
Chilton Didcot, Oxon OX11 0QX, England

Abstract

A leading order QCD analysis of spin asymmetries in polarized deep inelastic lepton nucleon scattering is presented within the framework of the radiative parton model. Two resulting sets of plausible leading order spin dependent parton distributions are presented, respecting the fundamental positivity constraints down to the low resolution scale $Q^2 = \mu_{LO}^2 = 0.23$ GeV^2. The Q^2 dependence of the spin asymmetries $A_1^{p,n,d}(x, Q^2)$ is investigated in the range $1 \leq Q^2 \leq 20$ GeV^2 and shown to be non-negligible for x-values relevant for the analysis of present data and possibly forthcoming data at HERA.

The measurements of polarized deep inelastic lepton nucleon scattering yield direct information [1-3] on the spin-asymmetry

$$A_1^N(x,Q^2) \approx \frac{g_1^N(x,Q^2)}{F_1^N(x,Q^2)} = \frac{g_1^N(x,Q^2)}{F_2^N(x,Q^2)/\left[2x(1+R^N(x,Q^2))\right]} \quad , \tag{1}$$

$N = p, n$ and $d = (p+n)/2$, and $R \equiv F_L/2xF_1 = (F_2 - 2xF_1)/2xF_1$, where subdominant contributions have, as usual, been neglected. The leading order (LO) QCD parton model relates $A_1^N(x,Q^2)$ to the polarized $(\delta q^N, \delta\bar{q}^N)$ and unpolarized $(q^N, \bar{q}^N)$ quark distributions, where $q = u, d, s$, via

$$A_1^N(x,Q^2) = \frac{\sum_q e_q^2 \left[\delta q^N(x,Q^2) + \delta\bar{q}^N(x,Q^2)\right]}{\sum_q e_q^2 \left[q^N(x,Q^2) + \bar{q}^N(x,Q^2)\right]} \tag{2}$$

due to the fact that $2g_1 = \sum_q e_q^2(\delta q + \delta\bar{q})$, $2F_1 = \sum_q e_q^2(q+\bar{q})$ and $R = 0$ in LO (Callan-Gross relation). Henceforth we shall, as always, use the notation $\delta q^p \equiv \delta q$ and $q^p \equiv q$. The experimental results are often presented and theoretically analyzed in terms of $g_1^N(x,Q^2)$ extracted via the *measured* values of $A_1^N(x,Q^2)$, $F_2^N(x,Q^2)$ and $R^N(x,Q^2)$ according to eq. (1). Frequently also the assumption about the Q^2 independence of $A_1^N(x,Q^2)$ is employed in regions of x and Q^2 where it has not been experimentally tested. This assumption is, as is well known [3], *not* theoretically warranted since one expects different Q^2-evolutions of the numerator and the denominator due to the very different polarized and unpolarized splitting functions (except for $\delta P_{qq}^{(0)}(x) = P_{qq}^{(0)}(x)$), respectively, especially in the small-x region dominated by the flavor-singlet contributions.

It should be further noted that an analysis of $g_1^N(x,Q^2)$ as extracted from eq. (1) affords a full next-to-leading order (NLO) analysis due to the employed $R^N(x,Q^2) \neq 0$, typically of the order of $20 - 30\%$, and due to the fact that usually $2xF_1^N(x,Q^2)$ is well described only in a NLO QCD parton calculation since this latter quantity is typically about 20% smaller than the LO F_2^N. Such a NLO analysis is somewhat premature in view of the presently scarce and inaccurate data on $g_1^N(x,Q^2)$. Some further ambiguities supporting this attitude are the ones concerning flavor $SU(3)$ breaking effects, mentioned below, as well as those concerning the flavor singlet sector, in particular its gluonic component. For all these reasons it seems appropriate to apply first of all a LO analysis to the directly measured $A_1^N(x,Q^2)$ employing eq. (2), rather than to the derived $g_1^N(x,Q^2)$. Some further advantages of such an approach are that possible NLO and/or higher twist contributions are expected to partly cancel in the ratio of structure functions appearing in $A_1^N(x,Q^2)$, in contrast to the situation for $g_1^N(x,Q^2)$. Therefore we shall use all presently available data [2,4-8] in the small-x region where $Q^2 \gtrsim 1$ GeV^2 without bothering about lower cuts in Q^2 usually introduced in order to avoid possible nonperturbative higher twist effects as mandatory for analyzing $g_1^N(x, Q^2)$. It should be furthermore emphasized that, within a consistent LO analysis ($R^N = 0$, i.e. $2xF_1^N = F_2^N$), the results cannot be expected to agree with experimental extractions of $g_1^N(x, Q^2)$ better than to about 20%. Alas, the extracted polarized LO parton distributions are also reliable only to within about 20%. The analysis affords some well established set of unpolarized LO parton distributions which will be adopted from ref. [9].

The searched for polarized LO parton distributions $\delta f(x, Q^2)$, compatible with present data [2,4-8] on $A_1^N(x, Q^2)$, are constrained by the positivity requirements implying

$$|\delta f(x, Q^2)| \leq f(x, Q^2) \tag{3}$$

where $f = u, \bar{u}, d, \bar{d}, s, \bar{s}, g$, and furthermore by the sum rules

$$\Delta u + \Delta\bar{u} - \Delta d - \Delta\bar{d} = g_A = F + D = 1.2573 \pm 0.0028 \tag{4}$$

$$\Delta u + \Delta\bar{u} + \Delta d + \Delta\bar{d} - 2(\Delta s + \Delta\bar{s}) = 3F - D = 0.579 \pm 0.025 \tag{5}$$

with the first ($n = 1$) moment Δf defined by

$$\Delta f(Q^2) \equiv \int_0^1 dx \delta f(x, Q^2) \tag{6}$$

and the values of g_A and $3F - D$ taken from [10]. It should be noted that the first moment, i.e. the total polarization of each quark flavor Δq and $\Delta\bar{q}$ is conserved, i.e. Q^2-independent as a consequence of helicity conservation at the quark-gluon vertex [11], i.e. $\Delta P_{qq}^{(0)} \equiv \int_0^1 dx \delta P_{qq}^{(0)}(x) = 0$ and $\Delta P_{qg}^{(0)} = 0$. The constraint equations (4) and (5) are the ones used in most analyses performed so far. While the validity of the Bjørken g_A-sum-rule depends merely on the fundamental $SU(2)_f$ isospin rotation between matrix elements of charged and neutral axial currents, the constraint (5) depends critically on the assumed $SU(3)_f$ flavor symmetry between hyperon decay matrix elements of the flavor changing charged weak axial currents and the neutral ones relevant for $\Delta f(Q^2)$. We shall refer to the results based on the constraints (4) and (5) as the $SU(3)_f$ symmetric 'standard' scenario.

There are some serious objections [12] to this latter full $SU(3)_f$ symmetry. As a plausible alternative, Lipkin [13] has suggested a 'valence' scenario by assuming that the (flavor changing) hyperon β-decay data fix only the total helicity of *valence* quarks

$\Delta q_V \equiv \Delta q - \Delta\bar{q}$, i.e.

$$\begin{aligned}\Delta u_V - \Delta d_V &= g_A = 1.2573 \pm 0.0028 &(4')\\ \Delta u_V + \Delta d_V &= 3F - D = 0.579 \pm 0.025 &(5')\end{aligned}$$

by assuming only the fundamental $SU(2)_f$ isospin symmetry $u \leftrightarrow d$. We shall alternatively implement this extreme possibility in order to study the possible uncertainties, mentioned in the introduction, related to the $SU(3)_f$ symmetry breaking effects relevant for the $\Sigma^- \to n$ decay.

To understand the important (practical) difference between the above two scenarios, let us consider the quantity

$$\Gamma_1^{p,n}(Q^2) \equiv \int_0^1 dx g_1^{p,n}(x, Q^2) \qquad (7)$$

usually extracted [2,4-8] from measurements of $g_1^{p,n}(x, Q^2)$. In LO we have

$$\begin{aligned}\Gamma_1^{p,n}(Q^2) &= \pm\frac{1}{12}\Delta q_3 + \frac{1}{36}\Delta q_8 + \frac{1}{9}\Delta\Sigma\\ &= \pm\frac{1}{12}\Delta q_3 + \frac{5}{36}\Delta q_8 + \frac{1}{3}(\Delta s + \Delta\bar{s}) \qquad (8)\end{aligned}$$

with the flavor nonsinglet ($\Delta q_{3,8}$) and singlet ($\Delta\Sigma$) combinations being given by

$$\begin{aligned}\Delta q_3 &= \Delta u + \Delta\bar{u} - \Delta d - \Delta\bar{d}\\ \Delta q_8 &= \Delta u + \Delta\bar{u} + \Delta d + \Delta\bar{d} - 2(\Delta s + \Delta\bar{s}) \qquad (9)\\ \Delta\Sigma &= \sum_q(\Delta q + \Delta\bar{q}) = \Delta q_8 + 3(\Delta s + \Delta\bar{s}) \ .\end{aligned}$$

In the 'standard' scenario Δq_3 and Δq_8 are entirely fixed by eqs. (4,5) which gives for Γ_1^p, for example,

$$\Gamma_1^p = \frac{1}{12}(F + D) + \frac{5}{36}(3F - D) + \frac{1}{3}(\Delta s + \Delta\bar{s}) \ . \qquad (10)$$

For $\Delta s = \Delta\bar{s} = 0$ we recover the original estimate of Gourdin and Ellis and Jaffe [14], $\Gamma_{1,EJ}^p \approx 0.185$. Therefore we need[1] $\Delta s < 0$ in order to comply with recent experiments [4, 5] which typically give $\Gamma_1^p(Q^2 = 3 \text{ GeV}^2) \approx 0.12 - 0.13$. In the 'valence' scenario, only the valence contribution to Δq_8 is fixed by eq. (5'), with the entire Δq_3 still being fixed by (4') due to the assumption $\Delta\bar{u} = \Delta\bar{d} \equiv \Delta\bar{q}$, which gives for Γ_1^p in eq. (8)

$$\Gamma_1^p = \frac{1}{12}(F + D) + \frac{5}{36}(3F - D) + \frac{1}{18}(10\Delta\bar{q} + \Delta s + \Delta\bar{s}) \ . \qquad (11)$$

[1]In a LO analysis the polarized quark first moments should be considered as effective moments since in NLO their detailed physical interpretation depends on the convention (factorization scheme) adopted where possibly [15] $\Delta q \to \Delta q - (\alpha_s/4\pi)\Delta g$.

Thus, in contrast to eq. (10), a light polarized sea $\Delta\bar{q} < 0$ will account for the reduction of Γ_1^p as required by recent experiments [4, 5] *even* for the extreme $SU(3)_f$ broken choice $\Delta s = \Delta\bar{s} = 0$! We use this latter maximally $SU(3)_f$ broken polarized sea in our 'valence' scenario, eqs. (4') and (5'), which in addition is compatible with the $SU(3)_f$ broken unpolarized radiative input $s(x, \mu_{LO}^2) = 0$ of ref. [9]. A similar discussion holds for Γ_1^n and of course also for $g_1^{p,n}(x, Q^2)$.

Apart from applying the above scenarios for the polarized input distributions to $A_1^N(x, Q^2)$ rather than to $g_1^N(x, Q^2)$, the main ingredient of our analysis is the implementation of the constraint equation (3) down to [9] $Q^2 = \mu_{LO}^2 = 0.23$ GeV^2 which is *not* guaranteed in the usual studies done so far (recently, e.g. in [16-19]) restricted to $Q^2 \geq Q_0^2 = 1 - 4$ GeV^2. We follow here the radiative (dynamical) concept which resulted in the successful small-x predictions of unpolarized parton distributions as measured at HERA [9]. A further bonus of this analysis is the possibility to study the Q^2 dependence of $A_1^N(x, Q^2)$ in the small-x region over a wide range of Q^2 which might be also relevant for forthcoming polarized experiments (HERMES) at HERA. The results for the Q^2-dependence of $A_1^N(x, Q^2)$ are furthermore expected to hold almost unchanged also in the full NLO analysis due to the observed [9] perturbative stability of all the radiative model predictions for *measurable* quantities such as $F_2^p(x, Q^2)$.

Turning to the determination of the polarized LO parton distributions $\delta f(x, Q^2)$, it should be noted that $\delta g(x, Q^2)$ does not appear explicitly in the LO expression (2) and is therefore only weakly constrained by present data [1,2,4-8] on $A_1^N(x, Q^2)$ since it only enters indirectly via the Q^2-evolution equations. It is thus necessary to consider some reasonable constraints concerning $\delta g(x, Q^2)$ in particular in the relevant small-x region as, for example, requirements of color coherence of gluon couplings at $x \approx 0$ (equal partition of the hadron's momentum among its partons). This implies for the gluon and sea densities [20]

$$\frac{\delta f(x, Q_0^2)}{f(x, Q_0^2)} \sim x \qquad \text{as} \quad x \to 0 \ , \tag{12}$$

where the scale Q_0 at which this relation is supposed to hold remains unspecified. Although not strictly compelling, eq. (12) is expected [20] to hold at some 'intrinsic' bound-state-like scale ($Q_0^2 \lesssim 1$ GeV^2, say), but certainly not at much larger purely perturbative scales $Q_0^2 \gg 1$ GeV^2. Therefore we have fitted our input distributions at $Q_0^2 = \mu_{LO}^2 = 0.23$ GeV^2 using a general ansatz for the polarized (light) sea of the form $\delta\bar{q} \sim x^\alpha(1-x)^\beta \bar{q}$ with the result that all presently available asymmetry data require $\alpha \approx 0.9 - 1.1$ for both above scenarios. Consequently we have taken $\alpha = 1$ and assumed this power also to hold for $\delta g(x, \mu_{LO}^2)$, following eq. (12), although present data do not significantly constrain δg as will be discussed below. Our optimal LO distributions at $Q^2 = \mu_{LO}^2 = 0.23$ GeV^2 subject to the above constraints were found to be:

$$\begin{aligned}
\delta u_V(x, \mu_{LO}^2) &= 0.718 x^{0.2} u_V(x, \mu_{LO}^2) \\
\delta d_V(x, \mu_{LO}^2) &= -0.728 x^{0.39} d_V(x, \mu_{LO}^2) \\
\delta \bar{q}(x, \mu_{LO}^2) &= -2.018 x (1-x)^{0.3} \bar{q}(x, \mu_{LO}^2) \\
\delta s(x, \mu_{LO}^2) &= \delta \bar{s}(x, \mu_{LO}^2) = 0.72 \delta \bar{q}(x, \mu_{LO}^2) \\
\delta g(x, \mu_{LO}^2) &= 16.55 x (1-x)^{5.82} g(x, \mu_{LO}^2)
\end{aligned} \tag{13}$$

for the 'standard' scenario (corresponding to $\chi^2 = 98.4/92$ d.o.f.) respecting eqs. (4) and (5), while for the $SU(3)_f$ broken 'valence' scenario, based on the constraints (4') and (5'), we have:

$$\begin{aligned}
\delta u_V(x, \mu_{LO}^2) &= 0.726 x^{0.23} u_V(x, \mu_{LO}^2) \\
\delta d_V(x, \mu_{LO}^2) &= -0.668 x^{0.28} d_V(x, \mu_{LO}^2) \\
\delta \bar{q}(x, \mu_{LO}^2) &= -1.869 x (1-x)^{0.25} \bar{q}(x, \mu_{LO}^2) \\
\delta s(x, \mu_{LO}^2) &= \delta \bar{s}(x, \mu_{LO}^2) = 0 \\
\delta g(x, \mu_{LO}^2) &= 14 x (1-x)^{5.45} g(x, \mu_{LO}^2)
\end{aligned} \tag{13'}$$

which corresponds to $\chi^2 = 96.8/92$ d.o.f. The unpolarized input densities $f(x, \mu_{LO}^2)$ are taken from ref. [9] and, for obvious reasons, we have not taken into account any $SU(2)_f$ breaking ($\delta\bar{u} \neq \delta\bar{d}$) as is apparent from our ansatz for $\delta\bar{q} \equiv \delta\bar{u} = \delta\bar{d}$ proportional to $\bar{q} \equiv (\bar{u} + \bar{d})/2$ which should be considered as the reference light sea distribution for the positivity requirement (3). The fact that $\delta s(x, \mu_{LO}^2) \neq 0$ in (13) differs somewhat from our radiative input [9] $s(x, \mu_{LO}^2) = 0$, but for perturbatively relevant $Q^2 \gtrsim 0.8$ GeV^2, where the leading twist-2 dominates in the small-x region [9], the positivity inequality (3) is already satisfied. In this respect the input (13') for the 'valence' scenario, with the extreme $SU(3)_f$ breaking ansatz $\delta s(x, \mu_{LO}^2) = 0$, is more agreeable as far as our radiative (dynamical) approach is concerned. Furthermore $|\delta q_V(x, \mu_{LO}^2)| \sim q_V(x, \mu_{LO}^2)$ as $x \to 1$ in (13) and (13') which is also compatible with arguments based on helicity retention properties of perturbative QCD [20]. Finally, similarly agreeable fits to all present asymmetry data shown below (with a total χ^2 of 101 to 103 for 92 data points) can be also obtained for a fully saturated (inequality (3)) gluon input $\delta g(x, \mu_{LO}^2) = g(x, \mu_{LO}^2)$ as well as for the less saturated $\delta g(x, \mu_{LO}^2) = x g(x, \mu_{LO}^2)$. A purely dynamical [21] input $\delta g(x, \mu_{LO}^2) = 0$

is also compatible with present data, but such a choice seems to be unlikely in view of $\delta\bar{q}(x,\mu_{LO}^2) \neq 0$; it furthermore results in an unphysically steep [21] $\delta g(x, Q^2 > \mu_{LO}^2)$, being mainly concentrated in the very small-x region $x < 0.01$, as in the corresponding case [22, 23] for the unpolarized parton distributions in disagreement with experiment.

For calculating the evolutions of $\delta f(x,Q^2)$ to $Q^2 > \mu_{LO}^2$ we have used the well known LO solutions in Mellin n-moment space (see, e.g, refs. [23, 24]), with the moments of the polarized LO splitting functions given in [11]. These were then Mellin-inverted to Bjørken-x space as described, for example, in [23]. We have used $f = 3$ flavors when calculating $\delta P_{ij}^{(0)}$ and disregarded the marginal charm contribution to g_1^N stemming from the subprocess $\gamma^* g \to c\bar{c}$ [25]. The LO running coupling utilized was $\alpha_s(Q^2) = 4\pi/\beta_0 \ln(Q^2/\Lambda^2)$ with $\beta_0 = 11 - 2f/3$ and $\Lambda^{(f)}$ being given by [9]

$$\Lambda^{(3,4,5)} = 232, \;\; 200, \;\; 153 \;\; \text{MeV} \;\; .$$

The number of active flavors f in $\alpha_s(Q^2)$ was fixed by the number of quarks with $m_q^2 \leq Q^2$ taking $m_c = 1.5$ GeV and $m_b = 4.5$ GeV.

A comparison of our results with the data on $A_1^N(x,Q^2)$ is presented in fig.1. As already mentioned, fit results using a 'saturated' gluon $\delta g = g$ or $\delta g = xg$ at $Q^2 = \mu_{LO}^2$ are very similar to the ones shown in fig.1. Note that $A_1^N(x,Q^2) \to const.$ as $x \to 1$. The Q^2-dependence of $A_1^N(x,Q^2)$ is presented in fig.2 for some typical fixed x values for $1 \leq Q^2 \leq 20$ GeV^2. The predicted scale-violating Q^2-dependence is substantial and similar for the two rather different input scenarios (13) and (13'). In the (x,Q^2) region of present data [2,4-8], $A_1^p(x,Q^2)$ increases with Q^2 for $x > 0.01$. Therefore, since most present data in the small-x region correspond to small values of Q^2 ($\gtrsim 1$ GeV^2), the determination of $g_1^p(x,Q^2)$ at a larger fixed Q^2 (5 or 10 GeV^2, say) by assuming $A_1^p(x,Q^2)$ to be independent of Q^2, as is commonly done [2,4-8], is misleading and might lead to an *under*estimate of g_1^p by as much as about 20%, in particular in the small-x region. The situation is opposite, although less pronounced, for $-A_1^n(x,Q^2)$ shown in fig.2. This implies that $|g_1^n(x,Q^2)|$ might be *over*estimated at larger fixed Q^2 by assuming $A_1^n(x,Q^2)$, as measured at small Q^2, to be independent of Q^2. It should be emphasized that assuming $A_1(x,Q^2)$ to be *in*dependent of Q^2 *contradicts*, in general, perturbative QCD as soon as gluon and sea densities become relevant, due to the very different polarized and unpolarized splitting functions [11], $\delta P_{ij}^{(0)}(x)$ and $P_{ij}^{(0)}(x)$, respectively (except for $\delta P_{qq}^{(0)} = P_{qq}^{(0)}$ which dominates only in the large-x region). Moreover, the smaller x the stronger becomes the dependence of the exactly calculated $A_1(x,Q^2)$ on the precise form of the input at $Q^2 = \mu_{LO}^2$, as can be seen in fig.2 for $x = 10^{-3}$. For practical purposes, however, such ambiguities are irrelevant since, according to eq. (1), $A_1(x, Q^2) \approx 2xg_1/F_2 \to 0$ as $x \to 0$ is already unmeasurably small (of the order 10^{-3}) for $x \lesssim 10^{-3}$. Thus the small-x region is not accessible experimentally for $g_1(x, Q^2)$, in contrast to the situation for the unpolarized $F_{1,2}(x, Q^2)$. It is interesting to note that the (approximate) asymptotic ($x \to 0$) QCD expression [19, 26] for $A_1(x, Q^2)$ does not even qualitatively describe our exact LO results for $A_1(x, Q^2)$ in fig.2 for $x \geq 10^{-3}$.

In fig.3 we compare our LO results for $g_1^N(x, Q^2)$ with EMC, SMC and SLAC-E142/E143 data as well as with the fit 'A' of ref. [18]. Despite the fact that a LO analysis should not be expected to be more accurate than about 20%, as discussed at the beginning, the EMC [2] and E143 [5] 'data' at fixed values of Q^2 fall consistently below our results in the small-x region. This is partly an artefact of the LO approximation (i.e. $R^N = 0$ in eq. (1)) and partly due to the fact that the original small-x A_1^p-data at small Q^2 have been extrapolated [2, 5] to a larger fixed value of Q^2 by assuming $A_1^p(x, Q^2)$ to be independent of Q^2. According to the increase of A_1^p with Q^2 in fig.2, such an assumption underestimates g_1^p in the small-x region at larger Q^2. On the contrary, our results for $g_1^{p,d}$ do not show such a disagreement in the small-x region when compared with the SMC data [4, 6] in fig.3a where each data point corresponds to a different value of Q^2 since no attempt has been made to extrapolate $g_1^N(x, Q^2)$ to a fixed Q^2 from the originally measured $A_1^N(x, Q^2)$. Our predictions for the polarized LO parton distributions at the input scale $Q^2 = \mu_{LO}^2$ in eqs. (13) and (13') and at $Q^2 = 4$ GeV^2, as obtained from these inputs at $Q^2 = \mu_{LO}^2$ for the two scenarios considered, are shown in figs.4a and 4b, respectively. The polarized input densities in fig.4a are compared with our reference unpolarized LO dynamical input densities of ref. [9] which satisfy of course the positivity requirement (3) as is obvious from eqs. (13) and (13'). Our resulting polarized densities at $Q^2 = 4$ GeV^2 are compared with the ones (fit 'A') of ref. [18] in fig.4b. Since the polarized LO gluon density $\delta g(x, Q^2)$ is not strongly constrained by present experiments, we compare our gluons at $Q^2 = 4$ GeV^2 in fig.5 with the ones which originate from imposing extreme inputs at $Q_0^2 = \mu_{LO}^2$, such as $\delta g = g$, $\delta g = xg$ and $\delta g = 0$, instead of the one in (13') for the 'valence' scenario. The results are very similar if these extreme gluon-inputs are taken for the 'standard' scenario in (13), and the variation of $\delta g(x, Q^2)$ allowed by present experiments is indeed sizeable.

Finally let us turn to the first moments (total polarizations) $\Delta f(Q^2)$ of our polarized parton distributions, as defined in eq. (6). It should be recalled that, in contrast to $\Delta g(Q^2)$, the first moments of (anti)quark densities do not renormalize, i.e. are independent of Q^2, and thus the first moments implemented at the input scale $Q^2 = \mu_{LO}^2$ in (13) and (13') remain the same at any Q^2. Let us discuss the two scenarios in turn:

'standard' scenario: From the input distributions in (13) one infers

$$\Delta u_V = 0.9585, \quad \Delta d_V = -0.2988, \quad \Delta\bar{q} = -0.0720, \quad \Delta s = \Delta\bar{s} = -0.0519,$$
$$\Delta g(\mu_{LO}^2) = 0.444, \quad \Delta g(4\mathrm{GeV}^2) = 1.553, \quad \Delta g(10\mathrm{GeV}^2) = 1.915, \tag{14}$$

which result in $\Delta\Sigma = 0.268$. This gives, using eqs. (10) and (8),

$$\Gamma_1^p = 0.1506, \quad \Gamma_1^n = -0.0589 \quad , \tag{15}$$

which, for a LO result, is in satisfactory agreement with recent SMC measurements [4, 6]

$$\Gamma_1^p(10\mathrm{GeV}^2) = 0.142 \pm 0.008 \pm 0.011, \quad \Gamma_1^n(5\mathrm{GeV}^2) = -0.08 \pm 0.04 \pm 0.04 \tag{16}$$

as well as with the most recent E143 data [8] implying $\Gamma_1^n(2\mathrm{GeV}^2) = -0.037 \pm 0.008 \pm 0.011$.

'valence' scenario: From the input distributions in (13') one infers

$$\Delta u_V = 0.9181, \quad \Delta d_V = -0.3392, \quad \Delta\bar{q} = -0.0672, \quad \Delta s = \Delta\bar{s} = 0,$$
$$\Delta g(\mu_{LO}^2) = 0.417, \quad \Delta g(4\mathrm{GeV}^2) = 1.509, \quad \Delta g(10\mathrm{GeV}^2) = 1.866, \tag{14'}$$

which result in a total singlet contribution of $\Delta\Sigma = 0.31$. This gives, using eqs. (11) and (8),

$$\Gamma_1^p = 0.1478, \quad \Gamma_1^n = -0.0617 \quad , \tag{15'}$$

which again compares well with the experimental values in (16).

In both scenarios the Bjørken sum rule manifestly holds due to our constraints (4) and (4'), i.e. eq. (8) yields ($\Delta\bar{u} = \Delta\bar{d}$)

$$\Gamma_1^p(Q^2) - \Gamma_1^n(Q^2) = \frac{1}{6} g_A \quad . \tag{17}$$

It is also interesting to observe that at our low input scale $Q^2 = \mu_{LO}^2 = 0.23$ GeV^2 the nucleon's spin is, within 20%, carried by quarks and gluons, $\frac{1}{2}\Delta\Sigma + \Delta g(\mu_{LO}^2) \approx 0.57$, according to (14) and (14'), which implies for the helicity sum rule

$$\frac{1}{2} = \frac{1}{2}\Delta\Sigma + \Delta g(Q^2) + L_z(Q^2) \tag{18}$$

$L_z(\mu_{LO}^2) \approx 0$. The approximate vanishing of this latter nonperturbative angular momentum, being built up from the intrinsic k_T carried by partons, is intuitively expected for low (bound-state-like) scales but not for $Q^2 \gg \mu_{LO}^2$. From our results for the total gluon polarization $\Delta g(Q^2)$ in (14) and (14') it is also apparent that the Q^2-independent anomaly [15] contribution $-[\alpha_s(Q^2)/4\pi]\Delta g(Q^2) \approx -0.03$ could equally well serve[1] as the experimentally required negative contribution [27] to Γ_1^N in (8), instead of allowing for finite negative sea contributions Δs and $\Delta \bar{q}$ in eqs. (10) and (11), respectively. Such alternative factorization scheme scenarios cannot be decided on purely theoretical grounds, but nevertheless a consistent and convention independent analysis of the anomaly contribution in Bjørken-x space requires the full knowledge of all polarized two-loop splitting functions.

Finally let us remark that our results demonstrate the compatibility of our very restrictive radiative model, cf. eq. (3), down to $Q^2 = \mu_{LO}^2 = 0.23$ GeV^2, with present measurements of deep inelastic spin asymmetries. A FORTRAN package containing our optimally fitted 'standard' and 'valence' distributions can be obtained by electronic mail from vogelsang@v2.rl.ac.uk .

Acknowledgement

This work has been supported in part by the 'Bundesministerium für Forschung und Technologie', Bonn.

Note added

While this manuscript was being completed, a complete calculation of the two-loop splitting functions $\delta P_{ij}^{(1)}(x)$ in the $\overline{\mathrm{MS}}$ factorization scheme has appeared for the first time [28]. For the reasons stated in the introduction we postpone a full quantitative NLO analysis to a future separate publication.

References

[1] M.J. Alguard et al., SLAC-Yale Collab. (E80), Phys. Rev. Lett. **37**, 1261 (1976);
G. Baum et al., Phys. Rev. Lett. **45**, 2000 (1980);
G. Baum et al., SLAC-Yale Collab. (E130), Phys. Rev. Lett. **51**, 1135 (1983)

[2] J. Ashman et al., EMC, Phys. Lett. **B206**, 364 (1988); Nucl. Phys. **B328**, 1 (1989)

[3] For some recent discussions see, e.g., M. Anselmino, A. Efremov, and E. Leader, CERN-TH. 7216/94 (Phys. Rep., to appear);
G. Altarelli, P. Nason, and G. Ridolfi, Phys. Lett. **B320**, 152 (1994); Erratum **B325**, 538 (1994).

[4] D. Adams et al., SMC, Phys. Lett. **B329**, 399 (1994); Erratum **B339**, 332 (1994)

[5] K. Abe et al., SLAC-E143 Collab., Phys. Rev. Lett. **74**, 346 (1995) and SLAC-PUB-6508 (1994)

[6] B. Adeva et al., SMC, Phys. Lett. **B302**, 533 (1993);
J. Saborido, SMC, talk presented at the XXXth Rencontres de Moriond - QCD and High Energy Hadronic Interactions, Les Arcs, France, March 1995;
W. Wislicki, SMC, *priv. comm.*

[7] D.L. Anthony et al., SLAC-E142 Collab., Phys. Rev. Lett. **71**, 959 (1993);
F. Staley, SLAC-E142 Collab., Proc. of the Int. Europhysics Conf. on High Energy Physics, Marseille, France, 1993, eds. J. Carr and M. Perrottet, p.114

[8] K. Abe et al., SLAC-E143 Collab., SLAC-PUB-95-6734

[9] M. Glück, E. Reya, and A. Vogt, Univ. Dortmund DO-TH 94/24 and DESY 94-206 (Z. Phys. **C**, to appear)

[10] Particle Data Group, L. Montanet et al., Phys. Rev. **D50**, 1173 (1994);
F.E. Close and R.G. Roberts, Phys. Lett. **B316**, 165 (1993)

[11] G. Altarelli and G. Parisi, Nucl. Phys. **B126**, 298 (1977)

[12] L.M. Sehgal, Phys. Rev. **D10**, 1663 (1974); Erratum **D11**, 2016 (1975);
D.B. Kaplan and A. Manohar, Nucl. Phys. **B310**, 527 (1988);
M. Anselmino, B.L. Ioffe, and E. Leader, Sov. J. Nucl. Phys. **49**, 136 (1989);
H.J. Lipkin, Phys. Lett. **B230**, 135 (1989)

[13] H.J. Lipkin, Phys. Lett. **B256**, 284 (1991); **B337**, 157 (1994);
J. Lichtenstadt and H.J. Lipkin, Phys. Lett. **B353**, 119 (1995)

[14] M. Gourdin, Nucl. Phys. **B38**, 418 (1972);
J. Ellis and R.L. Jaffe, Phys. Rev. **D9** 1444 (1974); Erratum **D10**, 1669 (1974)

[15] G. Altarelli and G.G. Ross, Phys. Lett. **B212**, 391 (1988);
A.V. Efremov and O.V. Teryaev, Dubna report E2-88-287, 1988 [published in the Proceedings of the Int. Hadron Symposium, Bechyne, Czechoslovakia, 1988, eds. J. Fischer et al. (Czech. Academy of Science, Prague, 1989), p.302];
R.D. Carlitz, J.C. Collins, and A.H. Mueller, Phys. Lett. **B214**, 229 (1988)

[16] J. Ellis and M. Karliner, Phys. Lett. **B313**, 131 (1993)

[17] G. Altarelli, P. Nason, and G. Ridolfi, Phys. Lett. **B320**, 152 (1994); Erratum **B325**, 538 (1994)

[18] T. Gehrmann and W.J. Stirling, Z. Phys. **C65**, 461 (1995)

[19] R.D. Ball, S. Forte, and G. Ridolfi, CERN-TH/95-31

[20] S.J. Brodsky and I. Schmidt, Phys. Lett. **B234**, 144 (1990);
S.J. Brodsky, M. Burkhardt, and I. Schmidt, Nucl. Phys. **B441**, 197 (1995)

[21] M. Glück, E. Reya, and W. Vogelsang, Nucl. Phys. **B239**, 347 (1990)

[22] M. Glück, R.M. Godbole, and E. Reya, Z. Phys. **C41**, 667 (1989)

[23] M. Glück, E. Reya, and A. Vogt, Z. Phys. **C48**, 471 (1990)

[24] M. Glück and E. Reya, Phys. Rev. **D25**, 1211 (1982)

[25] M. Glück, E. Reya, and W. Vogelsang, Nucl. Phys. **B351**, 579 (1991)

[26] F.E. Close and R.G. Roberts, Phys. Lett. **B336**, 257 (1994)

[27] M. Glück and E. Reya, Phys. Lett. **B270**, 65 (1991)

[28] R. Mertig and W.L. van Neerven, Univ. Leiden INLO-PUB-6/95 and NIKHEF-H/95-031, June 1995

Figure Captions

Fig.1 Comparison of our results for $A_1^N(x, Q^2)$ as obtained from the fitted inputs at $Q^2 = \mu_{LO}^2$ for the 'standard' (eq.(13)) and 'valence' (eq.(13')) scenarios with present data [2,4-8]. Our results at different values of x correspond to different values of Q^2 according to experiment where each data point refers to a different value of Q^2, starting at $Q^2 \gtrsim 1$ GeV^2 at the lowest available x-bin.

Fig.2 The Q^2 dependence of $A_1^{p,n}(x, Q^2)$ as predicted by the LO QCD evolution at various fixed values of x.

Fig.3a Comparison of our 'standard' and 'valence' scenario results with the data [2,4-6] for $g_1^{p,d}(x, Q^2)$. The SMC data correspond to different $Q^2 \gtrsim 1$ GeV^2 for $x \geq 0.005$, as do the theoretical results; here the comparison with the GS fit [18] is limited to $x > 0.01$ since the data at lower x correspond to $Q^2 < 4$ GeV^2. The GS fit result for the E143 (g_1^p) data corresponds to a fixed $Q^2 = 4$ GeV^2.

Fig.3b Same as in fig.3a but for $g_1^n(x, Q^2)$. The E142 and E143 data [7, 8] correspond to an average $\langle Q^2 \rangle = 2$ and 3 GeV^2, respectively.

Fig.4a Comparison of our fitted 'standard' and 'valence' input densities in eqs. (13) and (13') with the unpolarized dynamical input densities of ref. [9].

Fig.4b The polarized densities at $Q^2 = 4$ GeV^2, as obtained from the input densities at $Q^2 = \mu_{LO}^2$ in fig.4a. The fitted GS (set A) densities of ref. [18] are shown for comparison.

Fig.5 The experimentally allowed range of polarized gluon densities at $Q^2 = 4$ GeV^2 for the 'valence' scenario with differently chosen $\delta g(x, \mu_{LO}^2)$ inputs. The 'fitted δg' curve is identical to the one in fig.4b and corresponds to $\delta g(x, \mu_{LO}^2)$ in eq. (13'). Very similar results are obtained if $\delta g(x, \mu_{LO}^2)$ is varied accordingly within the 'standard' scenario.

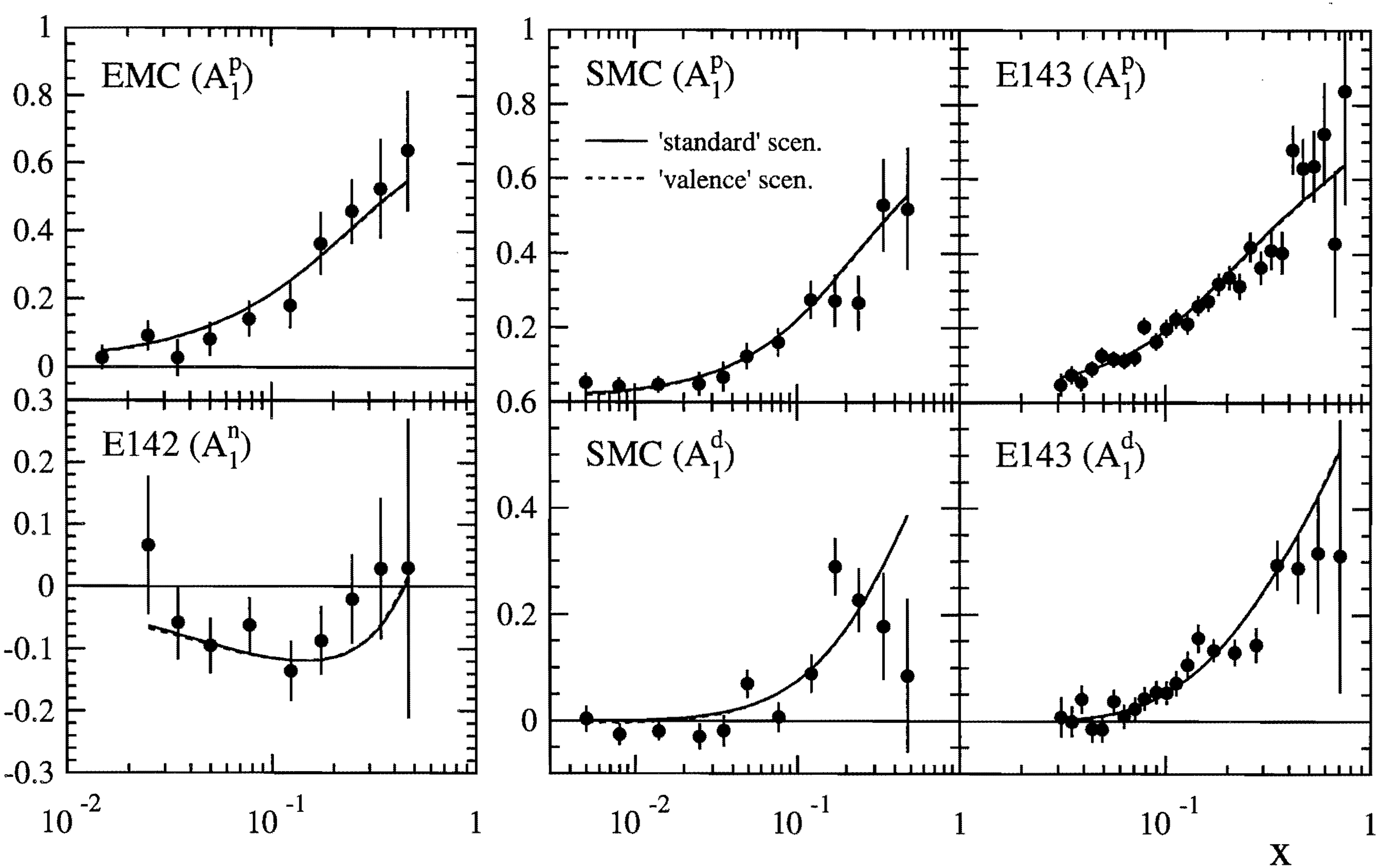
EMC (A_1^p)
SMC (A_1^p)
E143 (A_1^p)
E142 (A_1^n)
SMC (A_1^d)
E143 (A_1^d)
'standard' scen.
'valence' scen.
x

Fig. 1

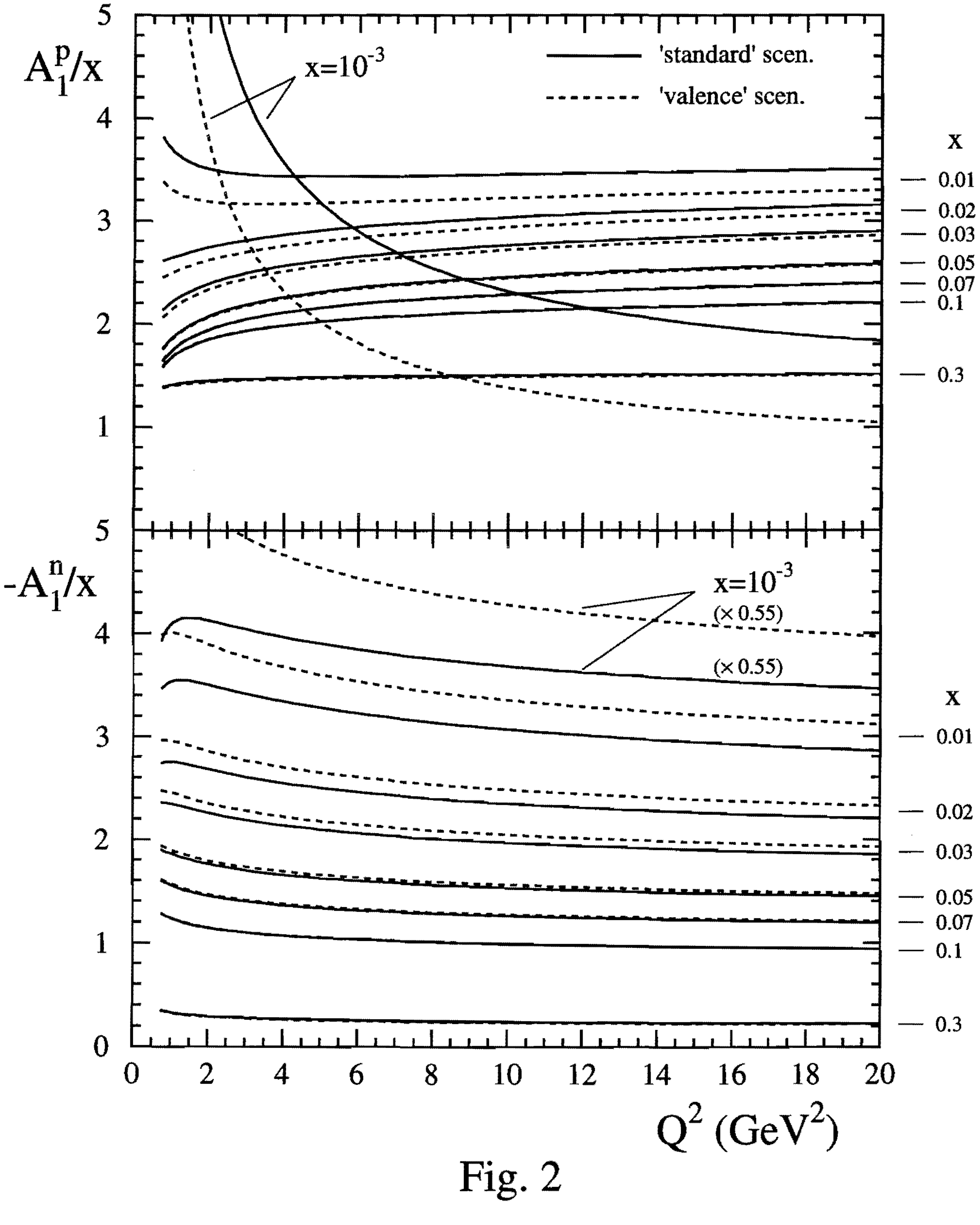

'standard' scen.
'valence' scen.
x=10^{-3}
A_1^p/x
x
0.01
0.02
0.03
0.05
0.07
0.1
0.3
$-A_1^n/x$
x=10^{-3}
(× 0.55)
(× 0.55)
x
0.01
0.02
0.03
0.05
0.07
0.1
0.3
Q^2 (GeV^2)

Fig. 2

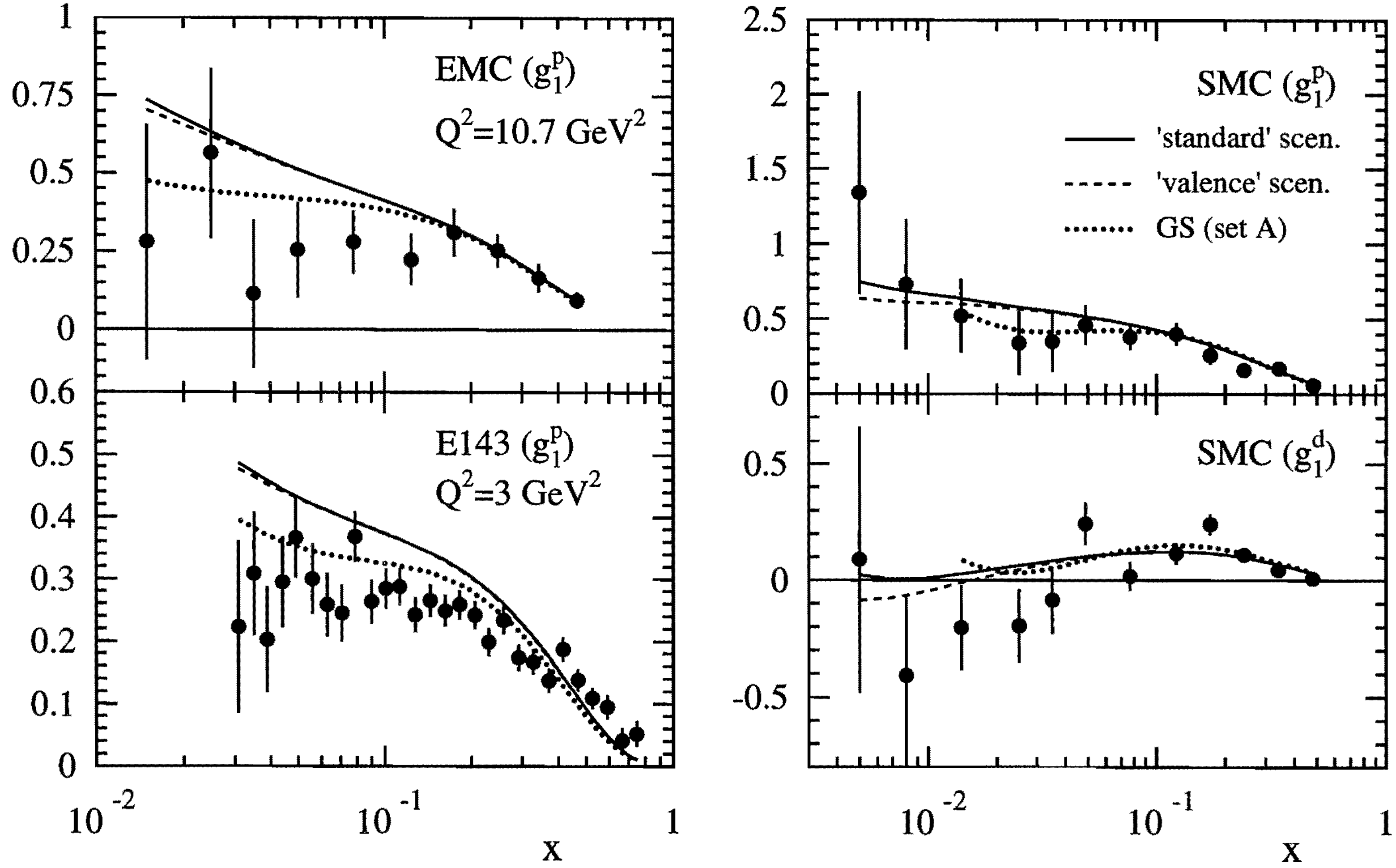

EMC (g_1^p)
Q^2=10.7 GeV^2
E143 (g_1^p)
Q^2=3 GeV^2
SMC (g_1^p)
'standard' scen.
'valence' scen.
GS (set A)
SMC (g_1^d)
1
0.75
0.5
0.25
0
0.6
0.5
0.4
0.3
0.2
0.1
0
2.5
2
1.5
1
0.5
0
0.5
0
-0.5
10^{-2}
10^{-1}
1
x

Fig. 3a

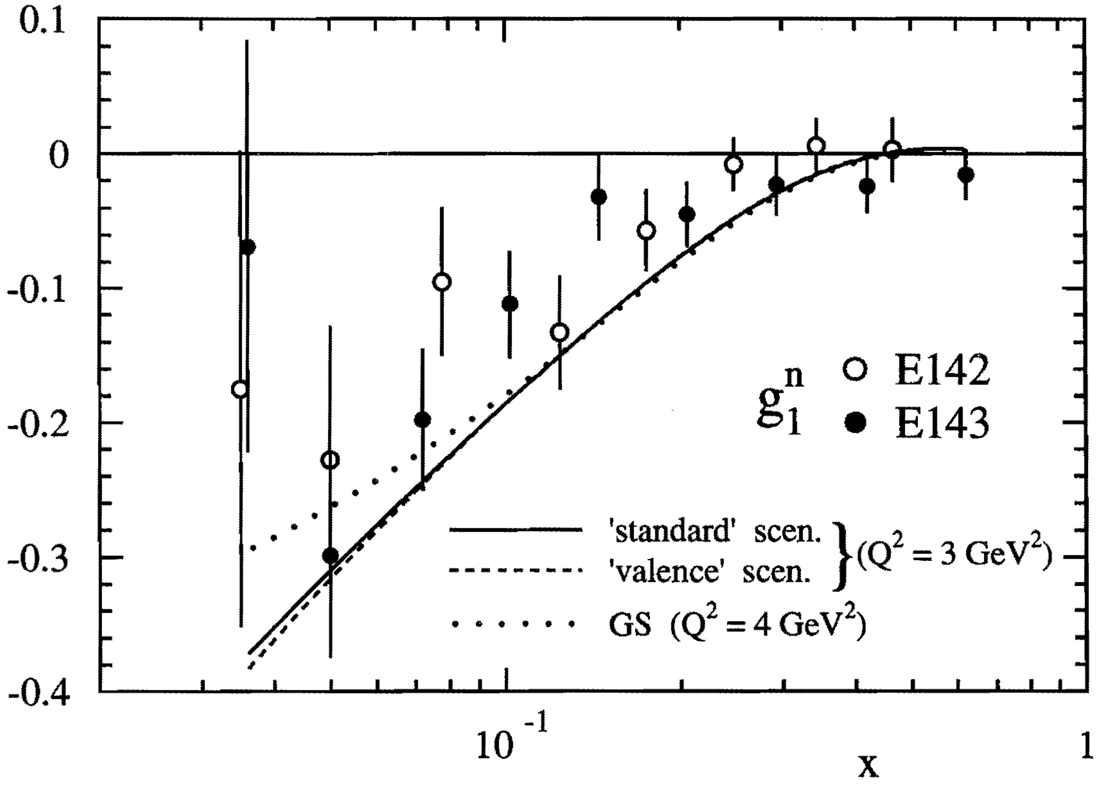
0.1
0
-0.1
-0.2
-0.3
-0.4
10^{-1}
1
x
g_1^n
E142
E143
'standard' scen.
'valence' scen.
($Q^2 = 3$ GeV^2)
GS ($Q^2 = 4$ GeV^2)

Fig. 3b

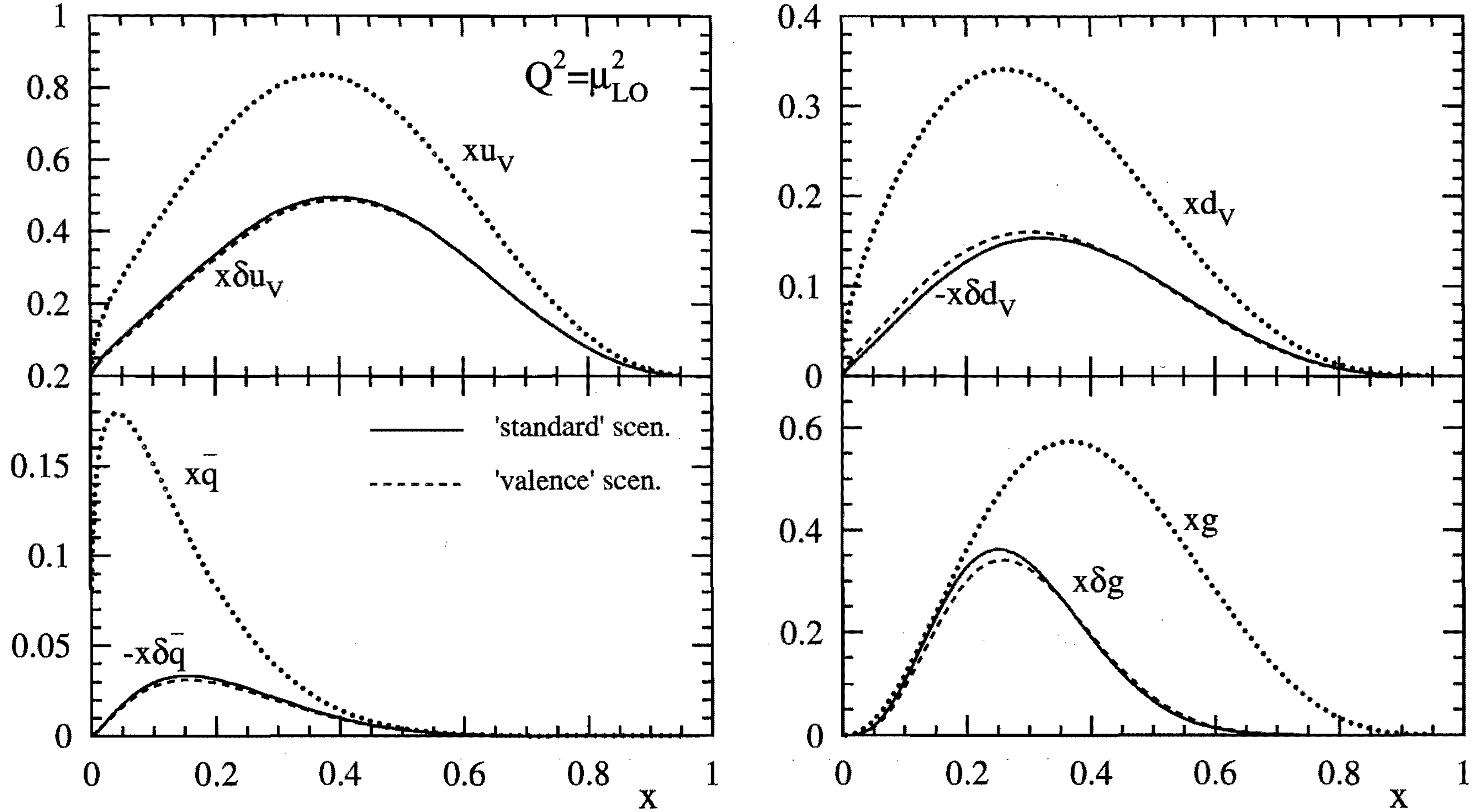

$Q^2=\mu^2_{LO}$
xu_V
$x\delta u_V$
xd_V
$-x\delta d_V$
$x\bar{q}$
$-x\delta\bar{q}$
'standard' scen.
'valence' scen.
xg
$x\delta g$
x
x

Fig. 4a

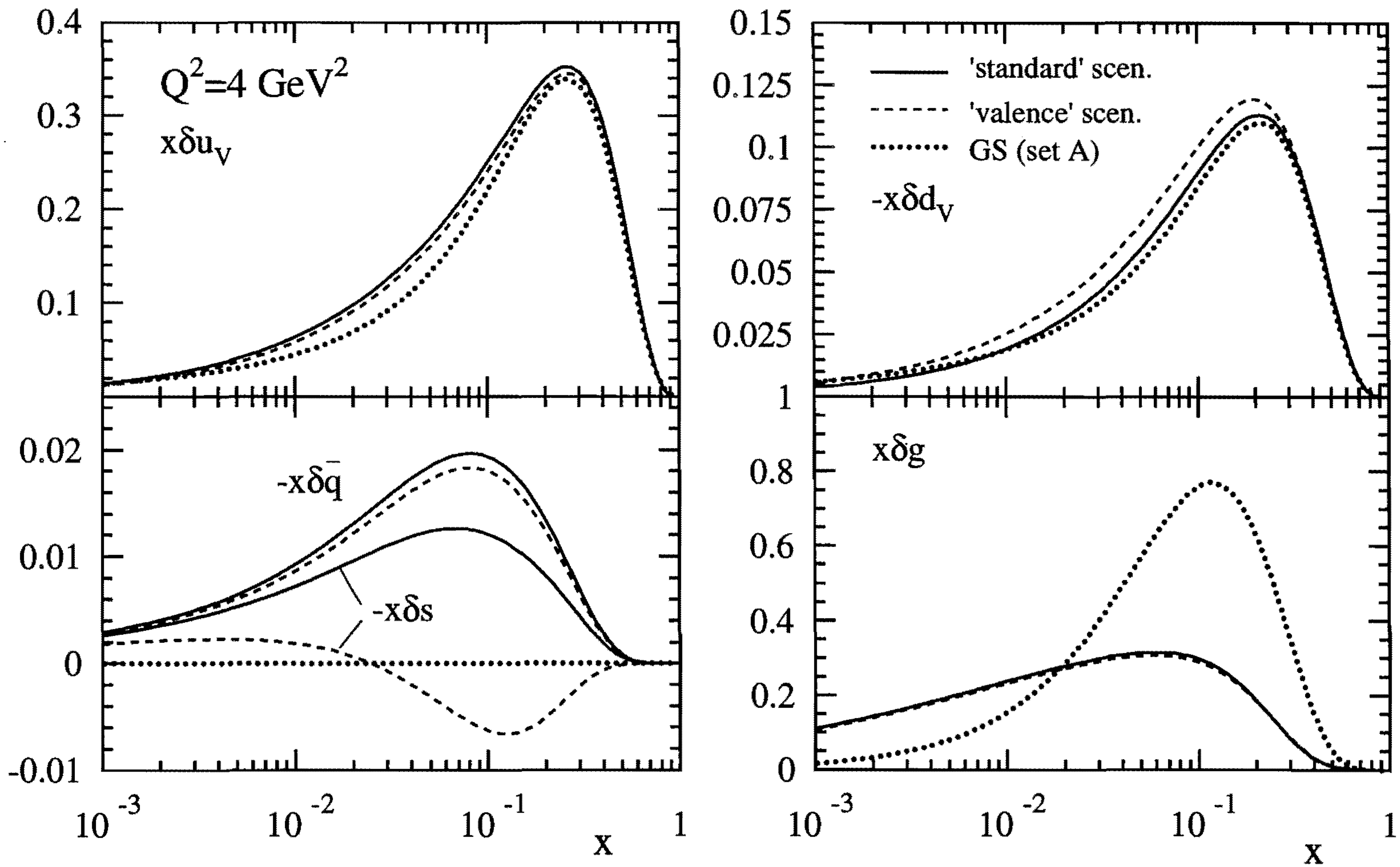

Q^2=4 GeV^2
$x\delta u_V$
$-x\delta d_V$
'standard' scen.
'valence' scen.
GS (set A)
$-x\delta\bar{q}$
$-x\delta s$
$x\delta g$
x

Fig. 4b

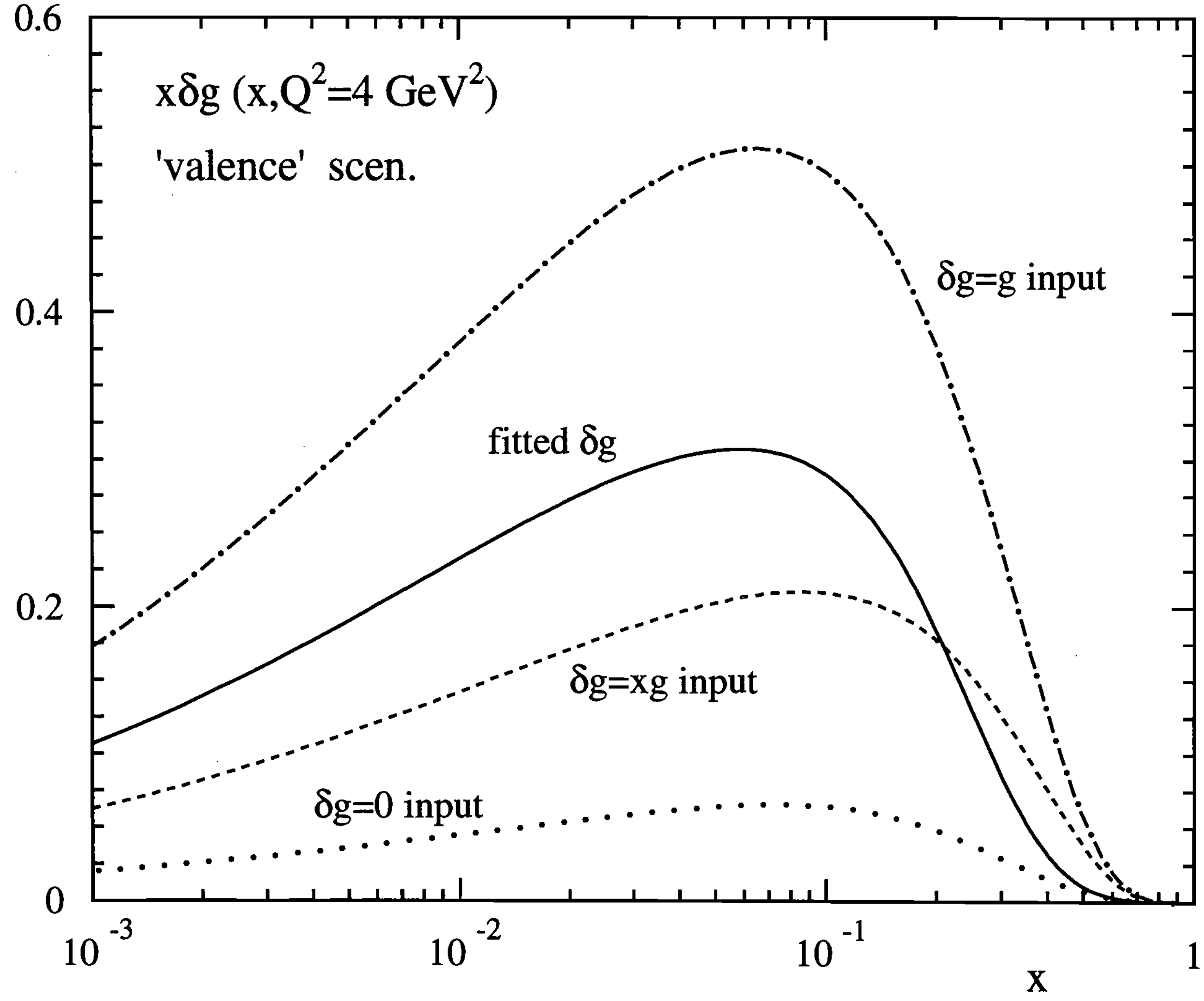
xδg (x,Q2=4 GeV2)
'valence' scen.
δg=g input
fitted δg
δg=xg input
δg=0 input
0.6
0.4
0.2
0
10 -3
10 -2
10 -1
1
x

Fig. 5